FOREST DRAGON 2: MID-TERM RESULTS OF THE EUROPEAN PARTNERS

C. Schmullius[(1)], J. Reiche[(1)], R. Leiterer[(1)], O. Cartus[(1)],
M. Santoro[(2)], U. Wegmüller[(2)],
Z.Y. Li[(3)], X. Tian[(3)], F.L.Ling[(3)],

[(1)] Department of Earth Observation, Friedrich-Schiller University Jena, Grietgasse 6, 07745 Jena, Germany;
Email: Johannes.Reiche, Reik.Leiterer, Oliver.Cartus, c.schmullius; @uni-jena.de
[(2)] Gamma Remote Sensing, Worbstrasse 225, 3073 Gümligen, Switzerland;
Email: santoro, wegmuller; @gamma-rs.ch
[(3)] Forest Remote Sensing Lab, Research Institute of Forest Resource Information Techniques, Chinese Academy of Forestry , Wanshoushan Hou, Haidian, 1000091 Beijing, China;
Email: zengyuan.li, tianxin, flling; @caf.ac.cn

ABSTRACT

One of the main objectives of the Forest DRAGON 2 project is the evaluation of the Forest DRAGON 1 large area forest growing stock volume (GSV) maps generated for Northeast and Southeast China, based on ERS-1/2 tandem coherence data from the mid 1990s. A special cross-comparison design mainly based on freely available Earth Observation products has been developed in consequence of lack of extensive in situ measurements. A reasonable agreement above 70 % between the forest GSV maps and the EO products in terms of forest/ non-forest could be achieved for NE and SE China. The assessment of forest cover and structure changes in China from the mid 1990s into the current decade is addressed by a pilot study at the regions of Daxinganling and Xiaoxinganling. A one-year stack (2007) of Envisat ASAR GMM data has been processed at 1-km pixel size with the BIOMASAR algorithm to obtain continuous GSV. Accordingly, the ERS-1/2 tandem data has been reprocessed to 1 km to allow an intercomparison of the two products, which in turn allowed observing scaling effects on the forest GSV. Preliminary results show plausible detection of forest cover changes.

1. INTRODUCTION

The forests of Northeast China and Southeast China, which represent one of the most important wood supplies in China, have been undergoing constant pressure for several decades. The existing forest resources are not considered adequate for the needs of the Chinese economy and livelihood of the Chinese people. The existing forest statistics in China differ significantly [1] and indicate a need to monitor the forests status and their development on a regular basis. This represents the background of the activities undertaken within Forest DRAGON 1 project and the ongoing follow-on project Forest DRAGON 2.

During the Forest DRAGON 1 project (2004 – 2008) forest growing stock volume (GSV) (also named stem volume) maps were produced for Northeast (~1,5 Million km²) and Southeast China (~3 Million km²) at 50 m spatial resolution from ERS-1/2 tandem coherence data (Fig. 1). The given ERS-1/2 tandem datasets consisted of 223 and 407 image pairs for Northeast and Southeast China respectively and were acquired under a wide range of meteorological conditions and perpendicular baselines (0 – 400m) in all seasons between 1995 and 1998. A new classification approach, based on synergy between the optical remote sensing product MODIS Vegetation Continuous Fields and ERS-1/2 tandem coherence has been developed for automatic and seasonal-adaptive retrieval of forest GSV, which is able to cope with multi-seasonal and multi-baseline data. The procedure integrates the semi-empirical Interferometric Water Cloud Model and discriminates between four GSV classes (0-20, 20-50, 50-80 and >80 m³/ha) [2]. The methodology will be hereafter referred to as DRAGON algorithm.

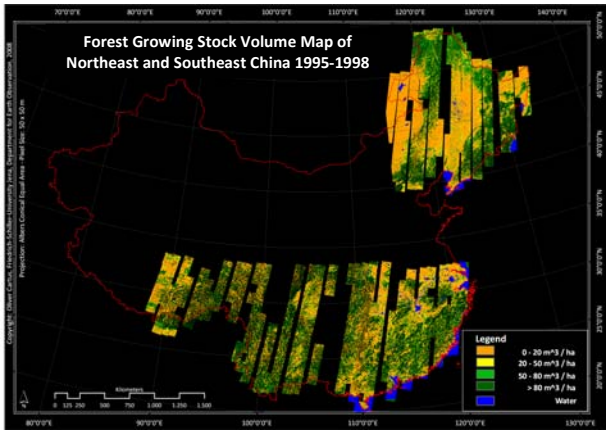

Figure 1. Forest GSV map of Northeast and Southeast China obtained from ERS-1/2 tandem coherence data for the years 1995 – 1998

Proc. 'Dragon 2 Programme Mid-Term Results 2008 – 2010', Guilin City, People's Republic of China
17–21 May 2010 (ESA SP-684, October 2010)

The evaluation of the large area forest GSV maps is a priority objective of the Forest DRAGON 2 project. For the validation a special cross-comparison design mainly based on freely available Earth Observation products had to be developed in consequence of lack of extensive in situ measurements.

The assessment of forest cover changes in China from the mid 1990s into the current decade is a further objective of the Forest DRAGON 2 project. For this scope and to further address the suitability of the Forest DRAGON products as potential input to global models (e.g. carbon models), it was decided to carry out a pilot study at the regions of Daxinganling (~200 x 200 km) and Xiaoxinganling (~300 x 300 km) in Northeast China. Due to the lack of a high-resolution product for the mid-2000 equivalent to the ERS-based map and the encouraging results on forest GSV retrieval from hyper-temporal Envisat ASAR ScanSAR data [3], it was decided to perform a comparison against GSV estimated from a one-year stack of Envisat ASAR images (Jan. 2007 – Feb. 2008) acquired in Global Monitoring Mode (GMM) at 1-km pixel size Accordingly, the ERS-1/2 tandem coherence data have been reprocessed to adhere to the coarse resolution of the ASAR GMM data, which in turn allowed observing scaling effects on the forest GSV.

The evaluation of the Forest DRAGON 1 map products is presented in Section 2. Section 3 describes the preliminary results of a pilot study at the regions of Daxinganling and Xiaoxinganling, analysing forest cover changes between the mid 1990s and 2007/08. A summarizing conclusion is finally given in Section 4.

2. CROSS-COMPARISON OF LARGE AREA FOREST GSV MAPS

In terms of implementing a robust accuracy assessment of different land cover datasets, [4] published the scientific state of the art in a 'best practice' document and [5] distinguished four approaches to a quantitatively estimation of the accuracies of land cover classifications: confidence values of the classifier, map comparison, cross-validation with training datasets and use of a robust spatial sampling design including ground reference information. Due to the lack of training datasets, ground references and robust classifiers, the comparison technique was applied in combination with a foregoing class harmonization [6].

For the comparison, several freely available global land cover products with different scale and observation periods have been used. Furthermore, it was possible to use the NLCD dataset of China as additional reference during the FSU work visit at the Chinese Academy of Forestry in 2009. Tab. 1 lists the different spatial and temporal resolution of each of the datasets used for the cross-comparison with the GSV map.

Table 1. Available land cover datasets

Product	Sensor	Resolution [km]	Year
LC AVHRR	AVHRR	1 x 1	1981 - 94
GLC2000	Spot	1 x 1	2000
VCF2000	MODIS	0.5 x 0.5	2000 / 2005
GlobCover	MERIS	0.3 x 0.3	2004 - 2006
NLCD	Landsat	0.05 x 0.05	1999

The AVHRR UMD land cover classification has been generated by the University of Maryland in 1998. Data from the AVHRR satellites acquired between 1981 and 1994 has been used to distinguish fourteen land cover classes [7]. The Global Land Cover 2000 (GLC2000) project is based on the VEGA 2000 dataset. This dataset consists of 14 months (1 Nov. 1999 – 31 Dec. 2000) of daily 1-km resolution satellite data acquired over the entire globe by the VEGETATION instrument on-board the SPOT 4 satellite [8]. The MODIS Vegetation Continuous Field Tree Cover product (VCF TreeCover) contains proportional estimates for the vegetation cover type woody vegetation for the year 2000. The product is derived from monthly composites of the 500 m MODIS sensor onboard NASA's Terra satellite. All seven MODIS bands were used to calculate the percentage tree cover [9]. GlobCover is an ESA initiative in cooperation with JRC, EEA, FAO, UNEP, GOFC-GOLD and IGBP. Based on ENVISAT MERIS 300m data global composites and land cover maps have been produced. The GlobCover service has been demonstrated over a period of 19 month (Dec. 2004 – Jun. 2006) for which a set of MERIS Full Resolution (FR) composites (bi-monthly and annual) and a Global Land Cover map are being produced [10]. The NLCD product was produced by the Chinese Academy of Sciences (CAS) by visual interpretation and digitization of satellite images including georeferenced and orthorectified Landsat TM and CBERS scenes from 1999 and 2000. A hierarchical classification system was applied and showed an overall accuracy greater than 90 % [11].

Comparing different thematic maps, such as the ERS-1/2 GSV map and a coarse resolution land cover product, implies having to face a number of issues related to spatial resolution and nomenclature. The comparison assessment was conducted at the spatial resolution of the single pixel of the ERS-1/2 GSV map (50 x 50 m). This allowed an exact comparison of the high resolution ERS-1/2 GSV dataset with the coarser

resolution land cover datasets without losing any thematic or spatial resolution. Problems occur when comparing the forest ERS-1/2 GSV map with ambiguous land cover classes, such as the *GlobCover* class '*Mosaic vegetation (grassland/shrubland/forest) (50-70%) / cropland (20-50%)*', because an agreement of the ambiguous land cover class with several ERS classes is possible. To enable a robust comparison method, each pixel of a finer scale product needed to be related unambiguously to a class of the coarser scale products. For the 500 x 500 m VCF product, there are no overlapping areas with the coarser scale 1000 x 1000 m products (AVHRR/ GLC2000). In contrast, for the 300 x 300 m GlobCover product such kind of areas are present. Each GlobCover pixel was analysed using a geospatial query, if the covered area only contain to one class of the coarser scale product. In the case of at least 2 classes, the relevant GlobCover pixels were masked out. Fig. 2 shows the conceptual approach of this method.

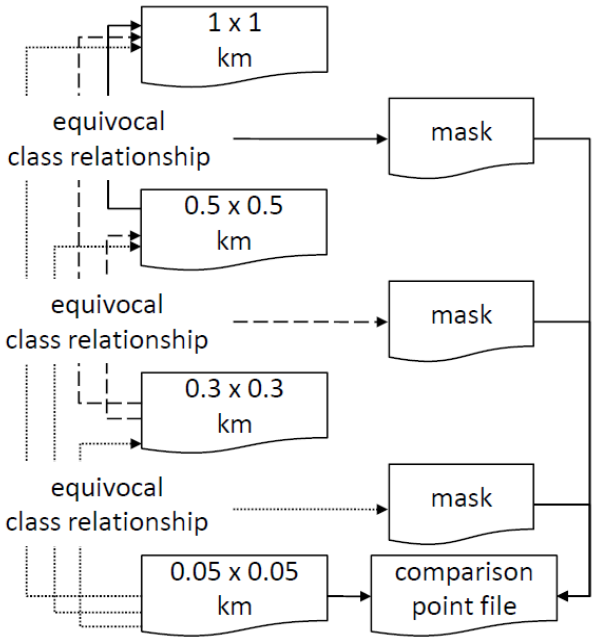

Figure 2. Intersection approach for a multi-scale comparison

The query with the VCF product was not essential due to the continuous values of the classification. Because there are no overlapping areas to coarser scale products for the 50 x 50 m products (NLCD/ GSV), a query similar to the GlobCover product is not necessary. According to this, only the unmasked areas were used for the comparison. This allows a robust comparison of the high resolution datasets with all of the coarser resolution land cover datasets.

2.1. Sample Design

The applied sampling design has been based on the FAO FRA2010 Sampling Design [12] and the Degree Confluence Project [13]. Latitude and longitude intersects (confluence points) were used to create a systematic sampling grid/design with an area of 10 km x 10 km covered by each sample site (Fig. 3).

Because the method described above is not fully robust when comparing the fuzzy described land cover classes and the GSV classes of the ERS-1/2 GSV product, the comparative assessment of the ERS-1/2 GSV maps with the different land cover classes has so far been conducted on the basis of forest and non-forest classes only. Hence, a reclassification using the LCCS concept for the legend harmonization, suggested by UNEP and FAO [9, 14], was accomplished. According to the FAO Forest Resources Assessment 2000, China's GSV averages 52 m³/ha [15]. Hence, the GSV map classes 3 (50-80 m³/ha) and 4 (> 80 m³/ha) have been aggregated as forest, whereas the other two classes have been defined as non forest. Further details on the reclassification are described in [16].

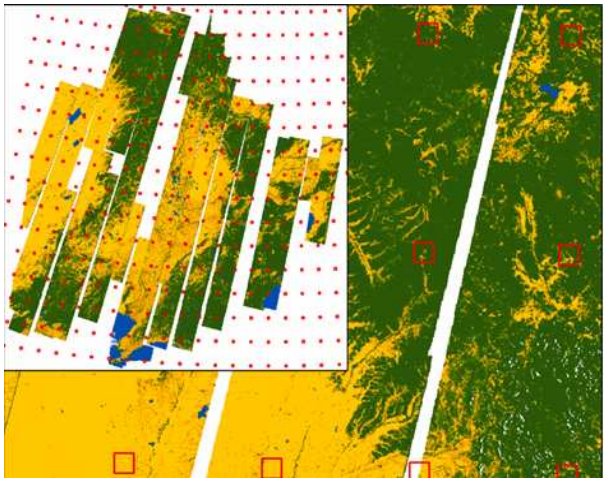

Figure 3. Example of Sample Plots with confluence centre points for Northeast China

2.2. Results

The results of this method are statistics, describing the correlation of the GSV product and the respective land cover product in terms of forest/ non-forest. The cross-comparison of the GSV map with the MODIS tree cover product (MOD44B) shows a very strong correlation of the distribution of the different GSV classes with the respective tree cover classes. The aggregated GSV forest class exhibits a coefficient of determination of 0.92, which indicates the solidness of the GSV classes. However, a reliable statement of the accuracy of the aggregated GSV product is not possible. The descriptive statistic analysis uses a 2D binning for the comparative

assessment and results in a correlation (difference/error) matrix. Based on this matrix the basic accuracy metrics *percentage of cases correctly allocated* (overall agreement) and the *cohen's kappa coefficient* (*kappa*) are derived (Fig. 4) [17].

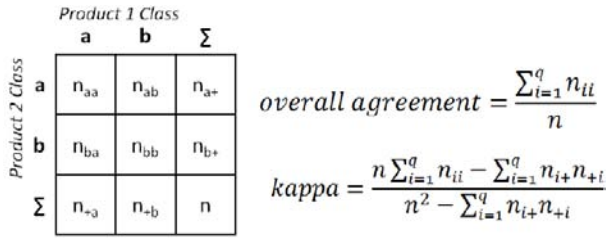

Figure 4. Correlation matrix and basic accuracy metrics

The GSV product features a reasonable agreement with all LC products, though, due to the moderate thematic accuracy of the coarser scale LC products a strong uncertainty remains (Tab. 2, Tab. 3).

Table 2. Overall agreement between the ERS-1/2 GSV map and the LC products for Northeast China based on aggregated forest/ non-forest classes

	OA	Cohen´s Kappa Coefficient
GSV vs. NLCD	0.79	0.55
GSV vs. GlobCover	0.74	0.49
GSV vs. VCF (>15% CC)	0.78	0.52
GSV vs. GLC2000	0.79	0.59
GSV vs. AVHRR LCC	0.77	0.51

Table 3. Overall agreement between the ERS-1/2 GSV map and the LC products for Southeast China based on aggregated forest/ non-forest classes

	OA	Cohen´s Kappa Coefficient
GSV vs. NLCD	0.68	0.33
GSV vs. GlobCover	0.74	0.43
GSV vs. VCF (>15% CC)	0.80	0.52
GSV vs. GLC2000	0.68	0.33
GSV vs. AVHRR LCC	0.68	0.32

The thematic information of the ERS-1/2 GSV map can be found within the LC products, which demonstrates the plausibility of the forest GSV classification. Furthermore, in areas where the ERS-1/2 GSV map and the LC products agree, the high resolution ERS-1/2 GSV product can provide information about the distribution of forest underneath the single coarse resolution LC pixel.

2.3. Forest GSV Accuracy Assessment

For the assessment of the individual ERS-1/2 forest GSV classes, the Chinese Academy of Forestry provided forest GSV reference data for a small test site located in the Changbai mountain range near the Chinese - North Korean border (43°09' N, 130°35' E) in the Jilin province. The region is characterised by hilly topography and mixed broad-leaved and Korea pine tree forest [18]. The forest GSV reference data was derived from airborne laser scanning (ALS) tree height estimates using allometry. The dataset was acquired during a campaign in 2009 and consists of 1521 point wise measurements covering an area of ca. 65 x 125 km. An overall accuracy of 79 % in terms of the four ERS-1/2 forest GSV classes has been achieved.

3. FOREST COVER CHANGE PILOT STUDY

To address the need to monitor the forest status and development in China on a regular basis, the assessment of forest cover and forest structure changes from the mid 1990s into the current decade has been declared as one of the main interests within the Forest DRAGON 2 project. Because of the lack of data equivalen to the ERS tandem data for the mid-2000s, it was decided to carry out a pilot study using hyper-temporal Envisat ASAR GMM data at 1 km pixel size at the regions of Daxinganling and Xiaoxinganling in Northeast China.

To retrieve forest GSV at the desired resolution of 1 km, using the DRAGON algorithm [2], it was required to reprocess the ERS-1/2 tandem coherence data (see Section 3.2). This in turn allowed observing different scaling effects on the forest GSV. The BIOMASAR algorithm [3] was instead used to process the stack of ASAR GMM images to obtain continuous estimates of forest GSV (see Section 3.3).

The intercomparison of the two map products will be done in terms of forest cover and forest structure changes. The intercomparison has not been concluded yet, however, an outlook is given in Section 4.

3.1. Study Area

The regions of Daxinganling (Greater Hinggan Mountains; 53°8' N, 123°4' E; ~200 x 200 km) and Xiaoxinganling (Lesser Hinggan Mountains; 47°10' N, 128°53' E; ~300 x 300 km) in Northeast China have been selected as the test area for the pilot study (Fig. 5). Daxinganling is characterised by gentle topography and needle-leaf forest dominated by larch trees. In 1987 a forest fire [19] widely destroyed the forest areas. The GSV is approximately 200 m³/ha. Xiaoxinganling is characterised by hilly terrain with an average slope of 10° and a low GSV, mostly below 200 m³/ha.

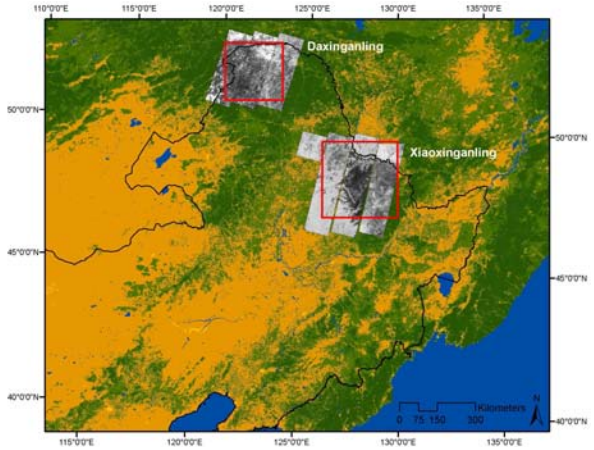

Figure 5. Location of the study regions of Daxinganling and Xiaoxinganling in Northeast China and the existing ERS-1/2 tandem data (interferometric SAR coherence) underlaid with the AVHRR Land Cover product

3.2. ERS-1/2 Tandem Coherence Forest GSV (1995 - 1997)

A multi-seasonal ERS-1/2 dataset was available, consisting of 9 and 13 tandem pairs for Daxinganling and Xiaoxinganling respectively. The data was acquired between winter 1995 and autumn 1997 and the perpendicular baselines varied between 60 and 352 m.

The methodology step consisted of interferometric processing of the ERS-1/2 tandem data to generate interferometric SAR coherence (Section 3.2.1) followed by model training and model inversion to retrieve forest GSV from the coherence (Section 3.2.2). Since the DRAGON algorithm [2] has only been applied at a 50 m resolution so far, scaling effects on the coherence estimates and on the retrieval were also investigated.

3.2.1. Interferometric Processing

Two basic approaches can be considered to process interferometric SAR coherence at 1 km scale for ERS-1/2 tandem images. The first approach considers the coherence estimation based on initially multi-looked (ML) ERS-1/2 images. To achieve an approximate pixel size of 1 km, ML factors of 40 in range and 200 in azimuth are used. The second approach consists of multi-looking the interferometric SAR coherence generated with a pixel spacing of 50 m (ML 2x10) with factors 20 and 20. Because the forest GSV is retrieved from coherence information, correct coherence estimation is essential for an accurate GSV retrieval. Both approaches have therefore been investigated with respect to scaling effects on the interferometric SAR coherence estimation.

The investigation was carried out for several ERS-1/2 tandem datasets located within the region of Xiaoxinganling and is summarized below using an example dataset (03/04 October 1997, Track 0461, Frame 2655) for illustration. Figure 6-1, 6-2 and 6-3 show the results obtained with the first method, where coherence images at 50 m (ML 2x10; estimation area (ea) 150 – 250 m), 500 m (ML 20x100; ea 1500 – 2500 m) and 1 km (ML 40x200; ea 3000 – 5000 m) are compared. The application of the second method, where the interferometric SAR coherence was initially processed to 50 m (ml 2x10, ea 150 – 250 m) and then multi-looked to achieve a final resolution of 500 m and 1 km, is illustrated in Figure 6-4 and 6-5.

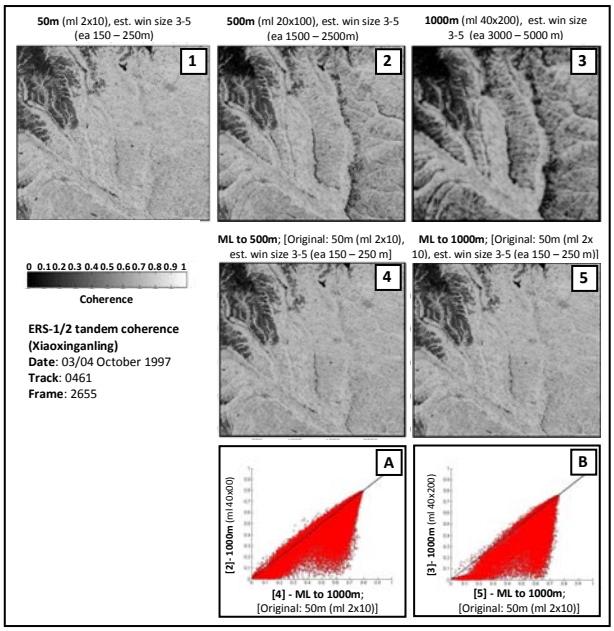

Figure 6. Interferometric SAR coherence variations of the two described estimation methods

The interferometric SAR coherence is estimated by averaging a number of pixels within a window to reduce the variance of the interferometric phase [20]. Due to coherent averaging over an area, low coherent areas lead to decreased coherence estimates in neighbouring regions. In particular, the first method is strongly affected by this effect as a result of the increasing coherence estimation area with decreasing pixel resolution (increasing ML factors) (Fig. 6-2 and 6-3). In consequence, this error would propagate into wrong GSV retrievals. Using the second method, this effect is minimized, since the coherence is estimated over a relatively small area (150 – 250 m) (Fig. 6-4 and 6-5) and then averaged. The scatter plots 6-A and 6-B show the correlation of both methods and highlight the clear underestimation of the interferometric SAR coherence by using the first method.

Based on these results, the second method was used for the interferometric processing of the ERS-1/2 tandem data, which is summarized below. The interferometric

processing was done on frame basis (100 x 100 km). It consisted of co-registration at sub-pixel level, multi-looking (2x10), common-band filtering and adaptive coherence estimation using window sizes between 3x3 and 5x5 pixels. For the common-band filtering SRTM-3 DEM data was included to consider effects in sloping areas [21]. All coherence and backscatter images were geocoded using SRTM-3 DEM data and resampled to a pixel size of 50 x 50 m. During the geocoding, maps of slope angle, layover/shadow, pixel normalization and local incidence angle were produced. Finally, the coherence was multi-looked with factors 20 and 20 to 1 km pixel size.

3.2.2. Model Training and Forest GSV Retrieval

The DRAGON algorithm used for the retrieval of forest GSV from coherence is based on the Interferometric Water Cloud Model (IWCM) [22]. The IWCM describes the coherence of a forest as a sum of a ground and a vegetation contribution. It includes five unknowns that should be determined via model training, which usually relies on the availability of forest inventory data [23, 24]. In [2] a model training approach that is independent from inventory data was developed by supporting the estimation of the unknown model parameters by means of the MODIS Vegetation Continuous Field (VCF) tree cover product [2]. The VCF product provides global sub-pixel estimates of tree cover at 500 m pixel size [9]. The clear relationship between the ERS-1/2 tandem interferometric SAR coherence and the VCF product allows the retrieval of four of the five model parameters from masking the coherence images for low (<10%) and high VCF (at least 70%) values. Respectively, γ_{gr} (ground coherence) and σ^0_{gr} (ground intensity) were estimated by masking areas low VCF values (<10%); γ_{veg} (ground coherence) and σ^0_{veg} (vegetation coherence) by masking areas of high VCF values (at least 70%). The remaining model parameter forest transmissivity β is set to 0.006 following the results on the estimation of this parameter using regression based model training with in situ data. For more details it is referred to [2].

The model training was conducted at 50 m resolution and then applied to the 1-km dataset to obtain the forest GSV. Since the model training is conducted on frame basis (100 x 100 km), the number of masked pixels representing areas of low and high VCF values strongly decreases at 1 km spatial resolution. Too few samples lead to an insufficient model estimate of γ_{gr} , σ^0_{gr}, γ_{veg} and σ^0_{veg} and hence to an inaccurate GSV retrieval.

For the VCF-based model training, a sufficient number of sample pixel for dense forest (VCF > 70 %) could be selected for most frames. In the case of too few sample pixels, the neighbouring frames have been included, which in turn enabled reasonable good model training results for the entire dataset. After the VCF-based model training at 50 m pixel spacing, the inversion of the model was carried out at the 1 km resolution. The retrieved GSV was then reparted in the four GSV classes (0-20, 20-50, 50-80 and >80 m³/ha). In addition, for each image frame, two flag images representing the percentage of 50 m water pixel and the percentage of 50 m pixel with valid/non-valid information in each 1 km pixel were generated (Fig. 7). As non-valid, pixels were labelled in case of layover and shadow and when they were masked during the model training due to strong spatial decorrelation. For details on the quality flag and masking procedure it is referred to [2]. The percentage of water underneath a 1 km pixel was used to classify water in a reprocessing step (percentage of water > 10 %). Finally, a nearest-neighbour interpolation with a window size of 3x3 was applied to fill gaps of non-valid 1 km pixel. The interpolation procedure is not applied if less then 5 pixel (50 %) of the interpolation window show no information (Fig. 7).

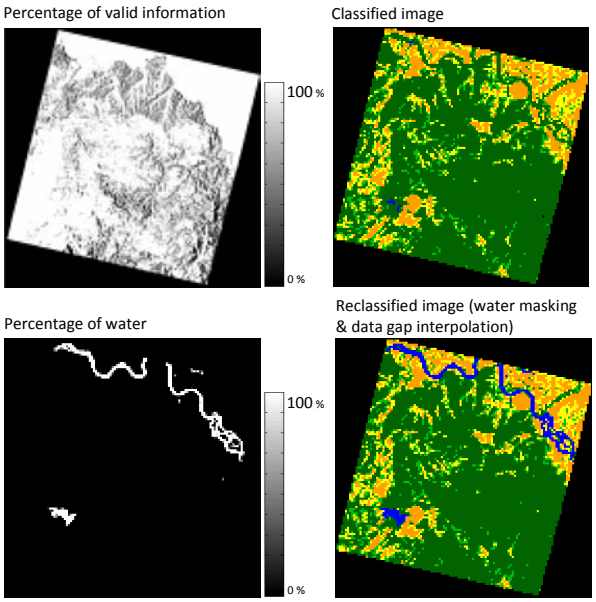

Figure 7. Classified image, corresponding flag files (perecentage of valid information & percentage of water) and the final reclassified image (09/10 Jan. 96, Track 418, Frame 2619)

Figure 8 shows the maps of forest GSV classes at 1 km pixel spacing for the regions of Daxinganling and Xiaoxinganling. It turned out that the described method (processing & interpolation) led to complete reduction of data gaps in mountainous regions, which is one of the major drawbacks of the 50 m ERS-1/2 forest GSV map [2].

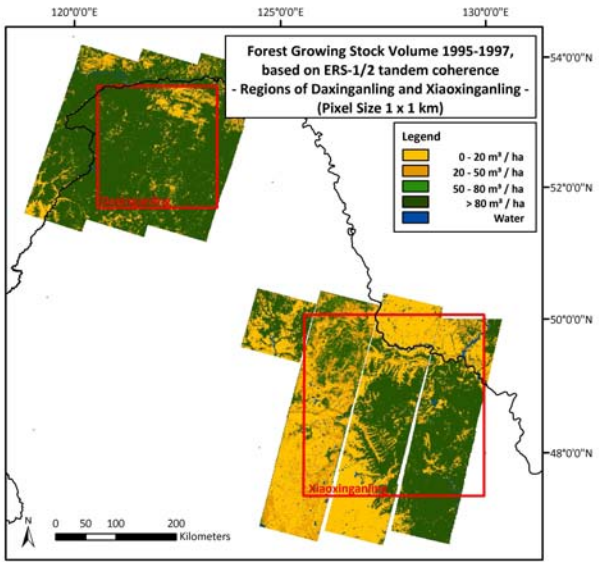

Figure 8. ERS-1/2 forest GSV 1995-1997 (1 km pixel size) of the regions of Daxinganling and Xiaoxinganling

The 1-km ERS-1/2 forest GSV map for Xiaoxinganling presented reasonable agreement with all LC products. Compared to the original 50 m ERS-1/2 forest GSV product, slightly higher values were obtained (Tab. 4). The reason for the slightly higher agreement are under investigation.

Table 4. Overall agreement between the GSV map at 50 m and 1 km pixel size and the LC products for Xiaoxinganling based on aggregated forest/ non-forest classes

	OA ERS-1/2 GSV 50m	OA ERS-1/2 GSV 1 km
NLCD	0.80	0.80
GlobCover	0.81	0.85
VCF (> 15% CC)	0.87	0.89
GLC2000	0.80	0.83
AVHRR LCC	0.65	0.67

3.3. Envisat ASAR GMM Forest GSV (2007/08)

Mapping of forest biophysical parameters with radar data acquired during the current decade can take advantage from data acquired by a wealth of spaceborne sensors. Nonetheless, repeated global coverage is only ensured by one of these, Envisat ASAR operating in ScanSAR mode. Since 2005 Envisat ASAR operates in the background mission the ScanSAR mode, i.e. continuous observations at either 100 or 500 meter whenever no data request has been posted to ESA. This allowed the generation of large stacks of hyper-temporal data also thanks to the large swath width (400 km). It is not uncommon that a point on the ground has been imaged more than 300 times during one year.

The drawback of Envisat ASAR backscatter observations for forest monitoring is the short wavelength (5.6 cm). It is well known that the sensitivity of the backscatter to forest parameters decreases when going from unvegetated to dense forest conditions. In the Forest DRAGON project Envisat ASAR images acquired in Alternating Polarization mode have been selected to derive forest information for the mid-2000 years in order to assess decadal forest cover changes with respect to the ERS-based GSV map. It was concluded that only forest/non-forest information can be obtained from the few observations available.

A number of studies have indicated that multi-temporal combination of estimates of GSV can lead to an improved estimate with respect to individual images [23, 25]. This concept has been applied in the recently developed BIOMASAR algorithm. In a similar manner to the DRAGON algorithm, a novel aspect of the BIOMASAR algorithm is the independence from in situ reference data for calibrating the model used to invert backscatter measurements for retrieving forest GSV.

The BIOMASAR algorithm [3, 26] consists of a SAR processing part that aims at achieving a stack of calibrated, geocoded and co-registered images at sub-pixel level. Then, for each backscatter measurement at a given pixel, a Water-Cloud type of model is trained using central tendency statistics, e,g. mean or mean value, of the backscatter for unvegetated areas and dense forest areas around the pixel of interest. Unvegetated areas and dense forests are selected by means of a measure of tree canopy cover, which is for example available in the MODIS Vegetation Continuous Fields tree canopy cover product [9]. It is here remarked that the VCF product is only used as mask to select backscatter values. Once the model has been trained, it is inverted and an estimate of GSV is obtained. The multi-temporal combination of individual GSV estimates consists of a weighted average, where the weights correspond to the backscatter difference between dense forest and unvegetated areas. In this way it is ensured that images presenting stronger sensitivity to GSV weight more than images characterized by only minor differences between the backscatter of open areas and dense forests. For details on the approach it is referred to [3, 26].

Analysis of the performance of the algorithm revealed the exceptional capability of the algorithm to retrieve forest GSV using Envisat ASAR ScanSAR data in the boreal zone (up to 300 m^3/ha) without apparent signs of saturation for the entire range of GSV found at several study areas [3, 26]. Images acquired under frozen dry

conditions were found to be most suitable for the retrieval. Accuracy of the order of 20-25% were achieved when aggregating full-resolution estimates with a factor 10 (i.e. for 1 and 10 km^2 pixel size starting from 100-m processed Wide Swath and 1-km processed Global Monitoring data, respectively).

Based on these encouraging results, the BIOMASAR algorithm has been applied to Envisat ASAR Global Monitoring Mode (GMM) data for the forest regions of Xiaoxinganling and Daxinganling in Northeast China with the aim of quantifying forest cover changes with respect to the mid-1990s. The available dataset consisted of a one-year stack of repeated ASAR GMM data acquired between January 2007 and February 2008. Figure 9 shows the ASAR GSV map for Xiaoxingaling (green tones) overlaid on the GLC2000 land-cover map.

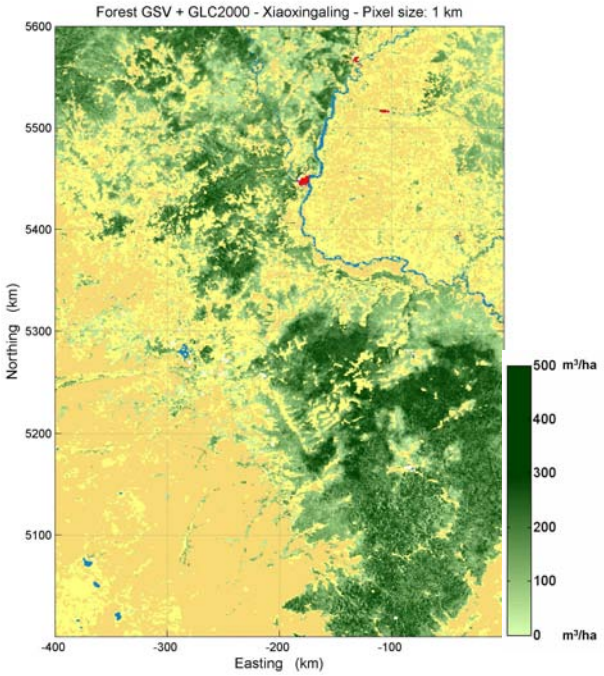

Figure 9. Continuous Envisat ASAR GMM GSV for the region of Xiaoxinganling. The ASAR data was acquired during 2007/08 and was processed to 1 km pixel size

The retrieval accuracy of the map is currently being investigated. A first analysis consisted in comparing the GSV values to the VCF canopy cover. Figure 10 shows a scatter plot of the BIOMASAR forest GSV (2007/08) and the VCF percentage tree cover 2005 (> 15%) for Xiaoxinganling. It appears that the VCF percentage tree cover saturates at ca. 100 m³/ha GSV, thus confirming the indications from several sites in the boreal zone [3] that radar observations are more related to forest structure, even at C-band.

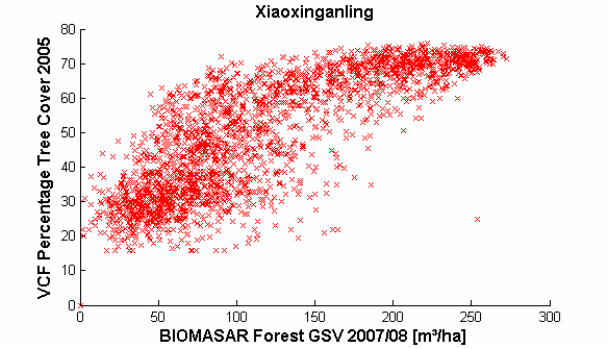

Figure 10. BIOMASAR forest GSV 2007/08 vs. VCF Percentage tree cover 2005 (Xiaoxinganling)

In order to allow an intercomparison with the forest ERS-1/2 GSV map of 1995-1997, the continuous forest GSV values have been reclassified into the four ERS-1/2 GSV classes (0-20, 20-50, 50-80 and >80 m³/ha) (Fig. 11).

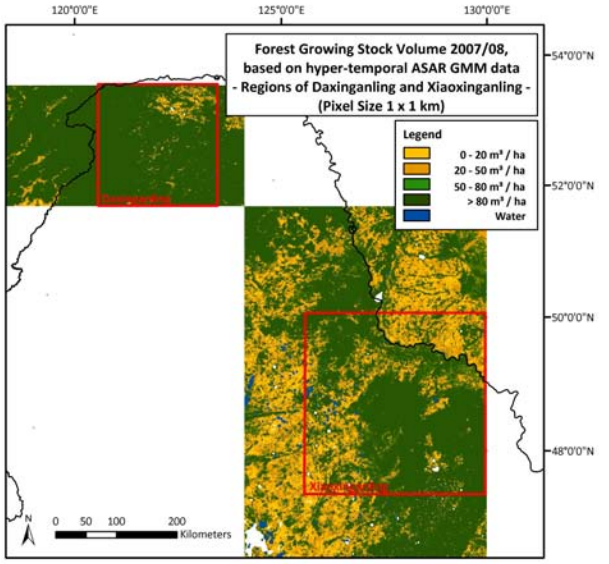

Figure 11. Envisat *ASAR GMM forest GSV 2007/08 (1 km pixel size) of the regions of Daxinganling and Xiaoxinganling reclassified to the four GSV classes used for the GSV retrieval using the ERS-1/2 tandem data*

4. CONCLUSION AND OUTLOOK

In this paper the Forest DRAGON 2 mid-term results of the European partners have been presented.

Validation of the ERS-1/2 GSV maps was still an open issue. An overall accuracy of 79% in terms of forest GSV using forest GSV inventory data at a small test site in Northeast China has now been obtained, thus highlighting the high performance of the GSV classification algorithm. For the evaluation of the large-

area forest GSV maps of Northeast and Southeast China generated during the Forest DRAGON 1 project, in addition a special cross-comparison scheme mainly based on freely available Earth Observation products was developed in consequence of lack of extensive in situ measurements. A reasonable agreement above 70 % between ERS-1/2 forest GSV map and the land cover datasets in terms of forest/ non-forest could be achieved for both Northeast and Southeast China. In consideration of factors that can affect accuracy, such as registration and legend conversion problems, the developed semi-automatic approach is completely transferable to other large-area investigation areas and is full adaptable for similar existing land cover data.

The second topic of the paper was a pilot study at the regions of Daxinganling and Xiaoxinganling in Northeast China to assess forest cover and forest structure changes in China from the mid 1990s into the current decade. The spatial resolution of the study was 1 km instead of the initial 50 m resolution of the original Forest DRAGON 1 map products. The limited information on forest parameters that can be achieved from the available Envisat ASAR data acquired at high resolution over China and the recent results on retrieval of forest GSV from hyper-temporal stacks of Envisat ASAR ScanSAR low resolution data justified this exercise. The ERS-1/2 tandem data (1995) have been reprocessed to 1 km resolution to adhere with the pixel size of Envisat ASAR Global Monitoring Mode data, which is widely available over China. This in turn allowed observing scaling effects on the forest GSV derived from the ERS coherence data. The major result in this sense is the reduction of topography-induced gaps in the GSV map. At 1-km pixel size, extreme topography is smoothened which allowed the retrieval of GSV also in those areas that at 50-m were severely affected by spatial decorrelation. The inter-comparison between the low-resolution GSV map and freely available land-cover products showed an agreement of the order if not slightly higher than for the 50-m case. A one year stack of Envisat ASAR GMM (2007-2008) data at 1-km pixel size has been processed, using the BIOMASAR algorithm. The accuracy assessment is ongoing. The plausibility of the retrieved GSV has been so far checked against the canopy cover information in the MODIS VCF product, revealing a significant agreement. Interestingly, the VCF estimates saturate at about 100 m^3/ha, which seems to indicate that the ASAR-based GSV contains more information on forest structure.

Preliminary analysis of the two forest GSV maps in terms of forest cover and structure change reveal patterns of both regrowth and deforestation. While plausible, the detected changes have not been confirmed yet. A major work of data and information collection and land-cover dynamics during the last decades is foreseen to be able to provide a detailed assessment of the detected changes

5. ACKNOWLEDGMENT

ESA and MOST are greatly acknowledged for establishing and managing the DRAGON and DRAGON 2 Programme. All Forest DRAGON project partners are acknowledged for cooperation. ERS and ASAR data were available through ESA Dragon AO C1P.2583 project.

References

1. Bull, G.Q. & Nilsson, S. (2004). An assessment of China's forest resources. *International Forestry Review*, **6**, 210-220.

2. Cartus, O., Santoro, M., Schmullius, C., Yong, P., Erxue, C. & Zengyuan, L. (2008). Creation of Large Area Forest Biomass Maps for Northeast China using ERS-1/2 Tandem Coherence. Proceedings of the Dragon 1 Programme Final Results 2004-2007, 21 – 25 April 2008, Beijing, ESA SP-655 (CD-Rom).

3. Santoro, M. & Cartus, O. (2010). STSE-BIOMASAR - Validating a novel biomass retrieval algorithm based on hyper-temporal Wide-Swath and Global Monitoring Envisat ASAR datasets, Final Report. ESA ESRIN contract No. 21892/08/I-EC, 2010.

4. Strahler, A.H., Boschetti, L., Foody, G.M., Friedl, M.A., Hansen, M.C., Herold, M., Mayaux, P., Morisette, J.T., Stehman, S.V. & Woodcock, C.E. (2006). Global Land Cover Validation: Recommendations for Evaluation and Accuracy Assessment of Global Land Cover Maps, Report of the Committee of Earth Observation (CEOS-WGCV).

5. Jung, M., Henkel, K., Herold, M. & Churkina, G. (2006). Exploiting synergies of global land cover products for carbon cycle modeling. *Remote Sensing of Environment*, **101**, 534–553.

6. Herold, M., Woodcock, C., Di Gregorio, A., Mayaux, P., Belward, A.S. & Lathan, J. (2006). A joint initiative for harmonization and validation of land cover datasets. *IEEE Transactions on Geoscience and Remote Sensing*, **44**(7), 1719–1727.

7. Hansen, M., DeFries, R., Townshend, J.R.G. & Sohlberg, R. (2000). Global land cover classification at 1km resolution using a decision tree classifier. *International Journal of Remote Sensing*, **21**, 1331-1365.

8. Bartholmé, E. & Belward, A. (2005). GLC2000: a new approach to global land cover mapping from Earth observation data. *International Journal of Remote Sensing*, **26**(9), 1959-1977.

9. Hansen, M.C., DeFries, R.S., Townshend, J.R.G., Sohlberg, R., Dimiceli, C. & Carroll, M. (2002). Towards an operational MODIS continuous field of percent tree cover algorithm: Examples using AVHRR and MODIS data. *Remote Sensing of Environment*, **83**, 303-319.

10. GLOBCOVER 2008. Globcover Product Description Validation Report I2.1.

11. Liu, J., Liu, M., Deng, X., Zhuang, D., Zhang, Z. & Luo, D. (2002). The land use and land cover database and its relative studies in China. *Journal of Geographical Sciences*, **12**, 275-282.

12. Wilkie, M.L., Cumani, R., Martucci, A. & Latham, J. (2008). The Global Forest Resources Assessment 2010 In 'Terrestrial Observation of our Planet' (Eds. R. Seussa), FAO, Rome, 32-33.

13. Jarrett, A. (2008): Degree Confluence Project - http://confluence.org/.

14. Ahlqvist, O. (2008). In search for classification that support the dynamics of science – The FAO Land Cover Classification System and proposed modifications. *Environment and Planning B: Planning and Design*, **35**(1), 169-186.

15. Food and Agriculture Organization (FAO) (2000). Global forest resources assessment 2000, Main Report, FRA 2000, *Forestry Paper 140*, Rome, Italy.

16. Cartus, O., Reiche, J., Leiterer, R., Santoro, M., Schmullius, C. & Zengyuan, L. (2009). Generation and Cross-validation of large-area forest stem volume maps for Northeast and Southeast China, using ERS-1/2 tandem coherence. Proceedings of the 2009 ISDE 6 Symposium (CD-ROM),09 – 12 September 2009, Beijing, China.

17. Foody, G.M. (2002). Status of land cover classification accuracy assessment. *Remote Sensing of Environment*, **80**, 185– 201.

18. Wang, X. (2002). Present situation and prospects of forest ecological network in Jilin Province, China. *Journal of Forestry Research*, **13**(4), 323-326.

19. Wang, X., Tang, Z. & Fang, J. (2006). Climatic control on forests and tree species distribution in the forest region of Northeast China. *Journal of Integrative Plant Biology*, **48**(7) 778-789.

20. Madsen, S. N. & Zebker H.A. (1998). Imaging Radar Interferometry. In 'Principles & Application of Imaging Radar' (Eds. Henderson, F.L. & A.J. Lewis), New York: Wiley, 359-380.

21. Santoro, M., Werner, C., Wegmüller, U. & Cartus, O. (2007). Improving of interferometric SAR coherence estimates by slope-adaptive range common-band filtering. Proceedings of the IGARSS 2007 (CD-Rom).

22. Askne, J., Dammert, P.B.G., Ulander, L.M.H. & Smith, G. (1997). C-band repeat-pass interferometric SAR observations of the forest. *IEEE Transactions on Geoscience and Remote Sensing*, **35**, 25-35.

23. Santoro, M., Askne, J., Smith, G. & Fransson, J.E.S. (2002). Stem Volume Retrieval in Boreal Forests with ERS-1/2 Interferometry. *Remote Sensing of Environment*, **81**, 19-35.

24. Santoro, M., Shvidenko, A., Mccallum, I., Askne, J. & Schmullius, C. (2007) Properties of ERS-1/2 coherence in the Siberian boreal forest and implications for stem volume retrieval. *Remote Sensing of Environment*, **106**(2), 154-172.

25. Kurvonen, L., Pulliainen, J. & Hallikainen, M. (1999). Retrieval of biomass in boreal forests from multitemporal ERS-1 and JERS-1 SAR images. *IEEE Transactions on Geoscience and Remote Sensing*, **37**(1), 198-205.

26. Santoro, M., Beer, C., Shvidenko, A., McCallum, I., Wegmüller, U., Wiesmann, A. & Schmullius, C. (2007). Comparison of forest biomass estimates in Siberia using spaceborne SAR, inventory-based information and the LPJ Dynamic Global Vegetation Model. Proceedings of Envisat Symposium 2007 (CD-ROM), 23-27 April 2007, Montreaux, Switzerland.